Current Research in Food Science 9 (2024) 100812

Contents lists available at ScienceDirect

Current Research in Food Science

journal homepage: www.sciencedirect.com/journal/current-research-in-food-science

Comprehensive lipidomics study of basa catfish and sole fish using ultra-performance liquid chromatography Q-extractive orbitrap mass spectrometry for fish authenticity

Weibo Lu [a], Yunyan Li [a], Lijun Ge [a], Honghai Wang [a], Ting Liu [c], Qiaoling Zhao [c], Zhujun Mao [b], Jingjing Liang [e], Pingya Wang [c], Kang Chen [a], Jing Xue [a,**], Qing Shen [b,d,*]

[a] Collaborative Innovation Center of Seafood Deep Processing, Zhejiang Province Joint Key Laboratory of Aquatic Products Processing, Institute of Seafood, Zhejiang Gongshang University, Hangzhou, 310012, China
[b] Panvascular Diseases Research Center, The Quzhou Affiliated Hospital of Wenzhou Medical University, Quzhou People's Hospital, Quzhou, 324000, China
[c] Zhoushan Institute of Food & Drug Control, Zhoushan, China
[d] Laboratory of Food Nutrition and Clinical Research, Institute of Seafood, Zhejiang Gongshang University, Hangzhou, 310012, China
[e] Zhejiang Provincial Institute for Food and Drug Control, Hangzhou, 310052, China

ARTICLE INFO

Handling Editor: Dr. Xing Chen

Keywords:
Lipidomics
Adulteration
Basa catfish
Sole fish
Multivariate statistical analysis

ABSTRACT

The authenticity of fish products has become a widespread issue in markets due to substitution and false labeling. Lipidomics combined with chemometrics enables the fraudulence identification of food through the analysis of a large amount of data. This study utilized ultra-high-performance liquid chromatography (UHPLC)-QE Orbitrap MS technology to comprehensively analyze the lipidomics of commercially available basa catfish and sole fish. In positive and negative ion modes, a total of 779 lipid molecules from 21 lipid subclasses were detected, with phospholipid molecules being the most abundant, followed by glycerides molecules. Significant differences in the lipidome fingerprinting between the two fish species were observed. A total of 165 lipid molecules were screened out as discriminative features to distinguish between basa catfish and sole fish, such as TAG(16:0/16:0/18:1), PC (14:0/22:3), and TAG(16:1/18:1/18:1), etc. This study could provide valuable insights into authenticating aquatic products through comprehensive lipidomics analysis, contributing to quality control and consumer protection in the food industry.

1. Introduction

With the rapid development of the global economy and the quick increase in per capita income, residents' awareness of health-oriented consumption continues to grow. Seafood products, known for their high protein and low fat content, have gained wide popularity and the consumption of seafood products has been continuously increasing, leading to an expansion in the seafood market supply. However, in recent years, there have been frequent occurrences of food safety and quality issues related to seafood products, which have attracted significant attention from society (Dai et al., 2022). Fraudulent behavior is one of the major concerns in seafood product quality and safety, and common fraudulent practices were substandard products, false labeling, adulteration, illegal additives, and other deceptive practices (Hassoun et al., 2020). Seafood products come in a wide variety and have substantial differences in economic value due to variations in growth environments, nutritional content, and taste. However, some seafood products might have striking resemblances in appearance and odor, making it difficult for consumers to effectively discern and identify them (Chang et al., 2021). Unscrupulous businesses engage in fraudulent practices to pursue high profits, which not only infringes upon consumers' basic rights but also poses potential health risks. For the producers, the negative impact of these factors leads to a decrease in sales volume and selling prices, creating a negative impact on the seafood industry and even affecting industrial structure and economic development.

* Corresponding author. Panvascular Diseases Research Center, The Quzhou Affiliated Hospital of Wenzhou Medical University, Quzhou People's Hospital, Quzhou 324000, China.
** Corresponding author.
E-mail addresses: xuejing@zjgsu.edu.cn (J. Xue), leonqshen@163.com, sq@zjgsu.edu.cn (Q. Shen).

https://doi.org/10.1016/j.crfs.2024.100812
Received 18 April 2024; Received in revised form 23 June 2024; Accepted 17 July 2024
Available online 18 July 2024

In recent years, there has been a rapid growth in the Chinese market for basa catfish (*Pangasius bocourti*), primarily due to its high flesh yield and abundant availability (Sriket & La-ongnual, 2018). Basa catfish has tender and white flesh, without small bones, making it easy to digest. It is nutritionally rich and relatively affordable in price (Khor et al., 2021). It is expected that the consumption of basa catfish will continue to increase in the domestic market in the future (Wang and Hsieh, 2016). However, due to the difficulty for ordinary consumers to discern basa catfish from other fish, and the lack of a strong fishy taste after cooking, many unscrupulous businesses misrepresent it as expensive marine fish, such as sole fish (*Cynoglossus semilaevis Gunther*) and cod, for sale. Currently, there is confusion between basa catfish and sole fish in consumers' awareness. In the seafood market and restaurant industry, basa catfish is sold under the name of "sole fish", which damages the legitimate rights and interests of consumers. The fraudulent labeling of seafood products is not limited to specific fish species or particular regions or countries. In fact, it has become a worldwide phenomenon of widespread fish species fraud throughout the entire supply chain (Bosko et al., 2018). While high profits are certainly a driving factor, the deeper reason lies in the difficulty for ordinary consumers to authenticate the authenticity of the products, and the time-consuming and costly identification procedures required by various inspection agencies. Therefore, conducting research on identification methods and techniques from a professional standpoint becomes crucial.

Modern identification techniques encompass omics technologies, molecular biology techniques, chromatographic spectroscopy, and modern mass spectrometry techniques. These techniques offer advantages such as high sensitivity, simplicity of operation, and strong specificity. Omics technologies, in particular, demonstrate outstanding sensitivity and detection throughput compared to traditional identification methods (Dai and Shen, 2022). Building upon the advancements in genomics, proteomics, metabolomics, and transcriptomics, they have become effective tools for food traceability, authentication, and fraud detection (Böhme et al., 2019). Lipidomics, an important branch of metabolomics, has emerged as a novel field based on metabolomics. It primarily involves the comprehensive analysis of lipid molecules in organisms to reveal their functions and potential roles in various biological processes. Currently, lipidomics methods find wide applications in the analysis of lipids in food and the study of dietary lipid nutrition (Tietel et al., 2023). Similar to metabolomics, lipidomics can be classified into targeted and untargeted methods based on the analytical objectives. Targeted methods focus on analyzing specific lipid targets, while untargeted methods aim to analyze the comprehensive lipid profile in samples. Lipidomic analysis produces a vast amount of data, which can be used to establish predictive models using chemometrics for food traceability, food adulteration identification, safety assessment, and improvement of harmful lipid formation in food production and processing, thereby enhancing food quality (Rey et al., 2022; Navarro-Reig et al., 2018). The study of lipidomics relies on the support of high-throughput detection techniques. Currently, most lipidomics analysis platforms are still based on electrospray ionization (ESI) and tandem mass spectrometry (MS/MS) analysis. In addition, matrix-assisted laser desorption/ionization-mass spectrometry (MALDI-MS) (Engel et al., 2022) and novel ambient mass spectrometry techniques such as desorption ionization mass spectrometry and rapid evaporative ionization mass spectrometry also play significant roles in lipidomics research (Deng et al., 2020; Ma et al., 2021). Ultra-high-performance liquid chromatography (UHPLC)-QE Orbitrap MS possesses significant advantages compared to conventional LC-MS, including sufficient sensitivity, high resolution, high-quality accuracy, and powerful fragment ion scanning capabilities, enabling the identification of numerous lipid isomers (Xuan et al., 2018). In summary, these emerging techniques, represented by these identification technologies, can provide highly accurate authentication of seafood products on the market and demonstrate a great potential in countering fraudulent activities.

In this project, advanced UHPLC-QE Orbitrap MS technology will be employed for comprehensive lipidomic analysis of commercially available basa catfish and sole fish. The lipid compositions of the two fish species will undergo statistical analysis to screen the major differential lipid components. The research findings will provide technical support for the species identification of basa catfish and sole fish, ensuring consumer rights and food safety.

2. Materials and methods

2.1. Chemicals and reagents

Acetonitrile (ACN) and methanol (MeOH) of chromatographic grade were obtained from Merck (Darmstadt, Germany). Analytical grade 1,2-dichloroethane (1,2-dce), chloroform, methyl tert-butyl ether (MTBE), and acetone were purchased from Aladdin Chemical Co., Ltd. (Shanghai, China) for lipid extraction. Other chemicals and reagents, including sodium hydroxide (NaOH) and boron trifluoride (BF3), unless otherwise stated, were obtained from Huadong Chemical Co. (Hangzhou, China). The deionized water was purified by Milli-Q water system (Millipore, Bedford, MA, USA). Polytetrafluoroethylene (PTFE) 0.22 μm filters were sourced from Whatman (Maidstone, UK).

2.2. Sample preparation

The fillets of sole fish and basa catfish were purchased from a trustable local company (Freshhema, Hangzhou, Zhejiang). Edible abdominal muscles were collected and stored at −4 °C for subsequent experiments. Lipids were extracted using a modified MTBE method (Matyash et al., 2008). Approximately 1.25 g of fish meat was weighed into a 50 mL centrifuge tube, followed by the addition of 5 mL of water and 20 mL of extraction solvent mixture (MTBE:MeOH = 5:1). Steel beads were added, and the samples were subjected to 5 min of grinding and 20 min of ultrasonic extraction at a frequency of 20 kHz and power of 100W in an ice-water bath. The mixture was then allowed to stand for 45 min, followed by three cycles of repeated extraction. The samples were subsequently centrifuged at −4 °C and 6000 g for 10 min. The upper organic phase was collected and evaporated in a rotary evaporator with the temperature set at 50 °C. The dried samples were re-dissolved in a 1 mL dichloromethane solution containing 50% methanol. Subsequently, the solution was vortexed for 20 s and subjected to ultrasonic treatment in an ice-water bath for 10 min. The samples were centrifuged at 6000 g for 10 min, and 75 μL of the supernatant was filtered through a 0.22 μm membrane into an injection vial for subsequent analysis.

2.3. UHPLC-QE Orbitrap/MS parameters

The ultra-high-performance liquid chromatography (UHPLC) conditions used in this experiment involved an Agilent 1290 series UHPLC system equipped with a Phenomenex Kinetex C18 (2.1 × 100 mm, 1.7 μm) liquid chromatography column for the separation of lipid mixtures. The temperature of the sample tray and column were maintained at 4 °C and 55 °C, respectively. The mobile phase composition for liquid chromatography consisted of 40% water, 60% acetonitrile, and a mixture of 10 mmol/L ammonium formate. The mobile phase B was composed of a mixture of 10% acetonitrile and 90% isopropanol, with 50 mL of a 10 mmol/L ammonium formate aqueous solution added to every 1000 mL. A gradient elution program was utilized as follows: 0–1.0 min at 40% B, 1.0–12.0 min increasing from 40% to 100% B, 12.0–13.5 min at 100% B, 13.5–13.7 min decreasing from 100% to 40% B, and 13.7–18.0 min at 40% B. The flow rate of the mobile phase was set at 0.3 mL/min, and the injection volume was 2 μL for positive ion mode and 6 μL for negative ion mode.

The mass spectrometry analysis was performed using a Q-Exactive Orbitrap (QE) mass spectrometer (Thermo Fisher Scientific, Waltham,

MA, US) equipped with an electrospray ionization (ESI) source. The data-dependent acquisition (DDA) mode was used for MS/MS spectrum collection, controlled by the Xcalibur 4.0.27 acquisition software (Thermo, US). The mass scan range was set from *m/z* 100 to 1200 for both positive and negative ion modes. The instrument parameters were as follows: The sheath gas flow rate was set at 30 arb, the auxiliary gas flow rate was set at 10 arb, the capillary temperature was set at 400 °C for positive ion mode and 300 °C for negative ion mode, the full mass resolution was set at 70,000, the resolution for MS/MS was set at 17,500, the collision energy for negative ion mode was set at 15V/30V/45V, and the spray voltage was set at 5.0 kV for ESI^+ and −4.5 kV for ESI^- mode.

2.4. Statistical analysis

Replicates of 16 samples from both basa catfish and sole fish were analyzed. The XCMS software was utilized for processing the raw mass spectrometry data, which included peak identification, extraction, integration, and alignment. The data was then calculated for normalization and standard deviation with Microsoft Excel software. The obtained results were imported into SIMCA-P14.1 software for multivariate statistical analysis. Orthogonal partial least squares discriminant analysis (OPLS-DA) was employed to explore differences between groups based on known classifications. Differential lipids were selected using the Variable Importance in Projection (VIP) plot. The heatmaps were generated using TBtools software.

3. Results and discussion

3.1. Lipid classes in fish tissue

UHPLC-Q-Exactive-MS was employed to identify lipid molecular species in basa catfish and sole fish. The comprehensive lipid profiling was achieved by employing both positive and negative ion modes. As shown in Fig. 1A, a total of 396 lipid molecular species were detected in positive ion mode, while 383 lipid molecular species were detected in negative ion mode. Various lipid classes including phospholipids (PLs), sphingolipids (SPs), glycerolipids (GLs), ceramides (Cers), glucosylgalactosyl diacylglycerols (GlcADG), and fatty acids (FAs) were analyzed for basa catfish and sole fish (as shown in Fig. 1B–Table S1). Among these classes, PLs were the most abundant, with 344 species in basa catfish and 353 species in sole fish. Within the PL class, phosphatidylcholines (PCs) were the most abundant molecular species, with 135 species in basa catfish and 142 species in sole fish. GLs ranked as the second most abundant lipid class in both fish species, with 291 species in basa catfish and 308 species in sole fish. Other lipid classes such as SPs and free fatty acids (FFAs) were also detected, but in smaller quantities. These findings were consistent with previous studies indicating that PLs and GLs were the major lipid classes in fish tissue samples (Wang et al., 2019). GLs serve as intermediates for energy and lipid storage and also act as carriers for fatty acid transport, playing critical roles throughout the life cycle. PLs are essential components of cell membranes, and different forms of phospholipids can modulate membrane fluidity and permeability (Hachem and Nacir, 2022). The exact structure of lipid molecular could be identified on the basis of its MS, MS/MS spectra, the database LIPID MAPS (LIPID MAPS tools package), and the published literatures (Zink and Mangelsdorf, 2004). Take the ion of *m/z* 746.5130 ($[PE\text{-}H]^-$) as an example, the main fragment ions in its MS/MS spectrum (Fig. 2A) were *m/z* 327.2326, 283.2426 and 436.2818, which were corresponding to the $[R_2COO]^-$ (C22:6), $[R_2COO\text{–}CO_2]^-$ and $[M\text{-}R_2CH=C{=}O\text{–}H]^-$, respectively. Thus, the ion of *m/z* 746.5130 was identified as PE(O-16:1/22:6). In another case of the ion of *m/z* 968.7629 ([TAG (16:1/22:5/22:6) + $NH_4]^+$), its MS/MS spectrum was shown in Fig. 2B. The fragment ions of *m/z* 623.5009, 385.2740 and 311.2355, which were generated due to neutral loss of $R_{22:6}COOH + NH_3$ from $[M + NH_4]^+$, acyl chain ($[RC{=}O + 74]^+$) and acyl chain ($[RC{=}O]^+$), respectively.

3.2. Characterization of lipid molecular species

PLs are amphipathic molecules composed of a hydrophilic head group containing nitrogen or phosphorus (referred to as the polar head) and a hydrophobic (lipophilic) long alkyl chain (referred to as the nonpolar tail). PLs can be further classified into different classes, such as PC and phosphatidylethanolamine (PE), based on the different polar head groups (Stoica et al., 2022). PLs are important components of biological membranes and are considered essential nutrients due to their nutritional properties and physiological and biological functions. In this study, the molecular analysis of PLs in basa catfish and sole fish was conducted using the UHPLC-Q Exactive Orbitrap method. PLs ionize well in negative ion mode, and various PLs such as PC, PE, phosphatidylglycerol (PG), phosphatidylinositol (PI), phosphatidylserine (PS), phosphatidic acid (PA), and lysophosphatidylcholine (LPC) and lysophosphatidylethanolamine (LPE) as Lysophospholipids (LPLs) were detected in basa catfish and sole fish. The main phospholipid molecules in basa catfish and sole fish were presented in the heatmap (Fig. 3A). PE, as an important component of cell membranes, can regulate processes such as membrane fusion, division, and apoptosis. The content of PE in sole fish and basa catfish was considerable, with a total of 72 PEs detected, but the structures of PE in the two fish tissues were quite different. The most disparate PEs included PE(O-18:2/22:5), PE (O-16:1/22:6), PE(18:0/20:4), PE(16:0/22:6), PE(O-16:1/20:4), etc. PC,

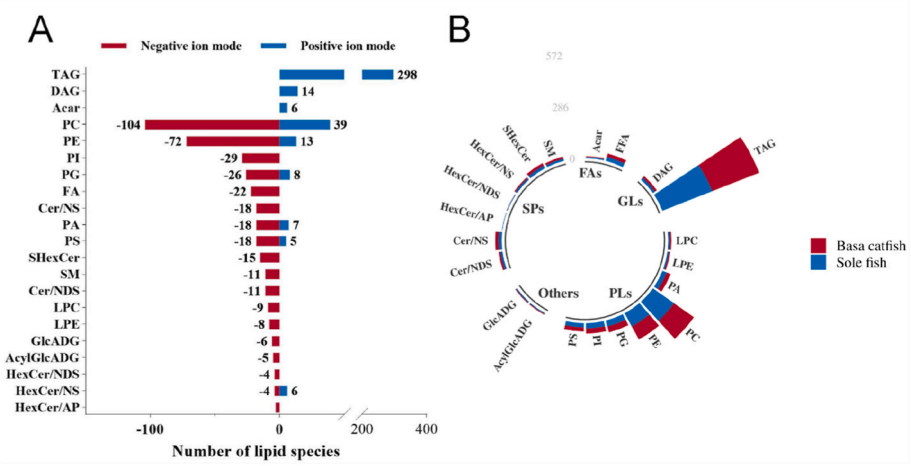

Fig. 1. (A) The number of lipid species detected in negative and positive ion mode; (B) the abundance of lipid species in basa catfish and sole fish.

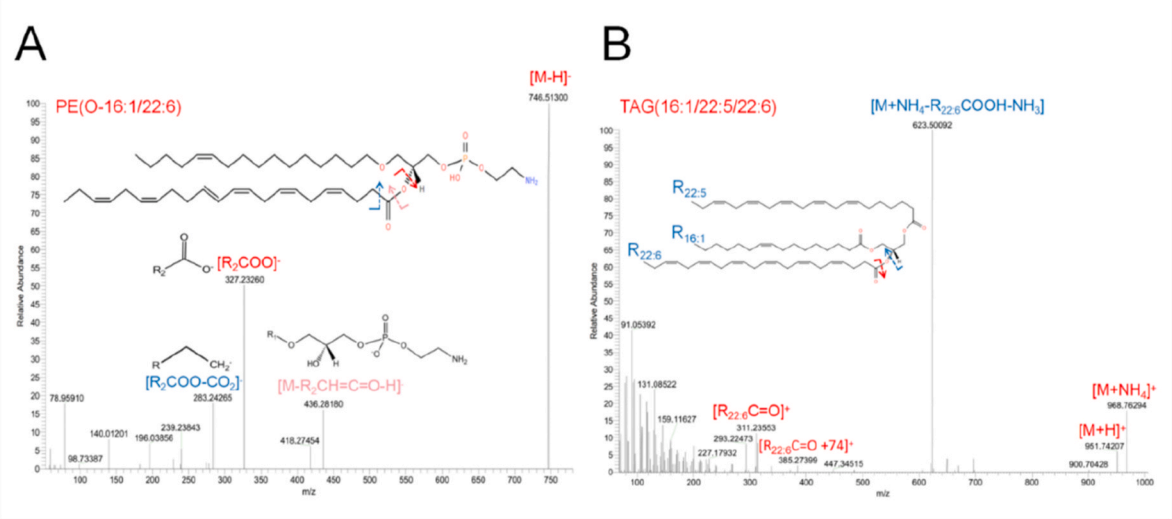

Fig. 2. The MS/MS spectra of PE(O-16:1/22:6) (A) and TAG(16:1/22:6/22:5) (B).

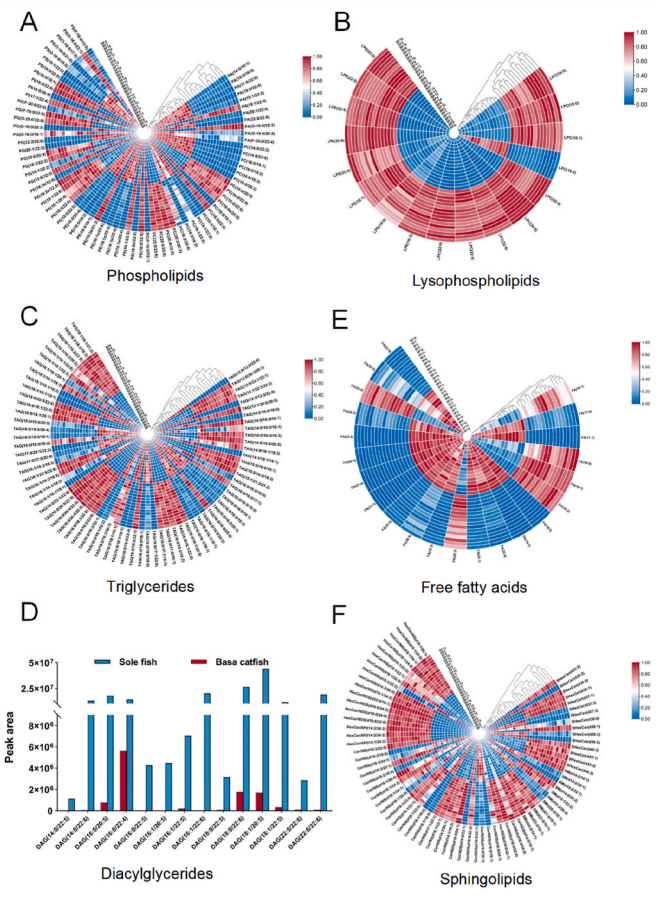

Fig. 3. The heatmap of main phospholipids (A), lysophospholipids (B), triglycerides (C), sphingolipids (D) and free fatty acids (F) in basa catfish and sole fish; (E) the peak area of all diacylglycerides in basa catfish and sole fish.

is an important participant in cell signal transduction and also a major component of lipoproteins. In basa catfish and sole fish, a total of 104 PCs were detected, and the two fish tissues showed different characteristics in PC's chemical structure. The most abundant PCs in basa catfish were PC(16:0/18:2), PC(18:1/18:1), PC(16:0/16:1), etc., while sole fish exhibited a structure with more polyunsaturated PCs, such as PC(16:0/20:5), PC(16:0/22:6), etc. Additionally, sole fish also exhibited higher levels of PCs with both chains being long-chain PUFAs, such as PC (22:6/22:6). Other PLs included 29 species of PI, 26 species of PG, 18 species of PS, and 18 species of PA. The overall chemical structure and content characteristics of these four classes of PLs were similar to PC and PE. Furthermore, 9 species of LPCs and 8 species of LPEs were detected in basa catfish and sole fish. LPC, as an important signaling molecule, can regulate cell proliferation in organisms. It has been found that the content of LPC is significantly reduced in obese and insulin-resistant animals, and it is believed that LPC can increase the expression of GLUT4 on cell membranes, thereby positively regulating the uptake of glucose by adipose tissue (Law et al., 2019; Bellot et al., 2023). As shown in heatmap of LPLs (Fig. 3B), the content of these two types of LPLs in sole fish was significantly higher than that in basa catfish. Similarly, the predominant fatty acid chains were C16:0, C18:1, C20:5, C22:5, and C22:6. Fish, flaxseeds, and certain nuts (such as walnuts) are considered good sources of omega-3 PUFAs. It has been reported that among PUFAs, particularly docosahexaenoic acid (DHA) and eicosapentaenoic acid (EPA), were considered effective antioxidants with neuroprotective activities that can reduce the risk of cardiovascular diseases (Shahidi and Ambigaipalan, 2018; Innes and Calder, 2020). In the published literatures, compared to other meat and milk, fish exhibited a higher proportion of unsaturated fatty acids, which were found to be good sources of supplementation (Li et al., 2017).

GLs is one of the most abundant lipid classes in living organisms. GLs were detected only in the positive ion mode in this study, with two major classes observed: triglycerides (TAGs) and diacylglycerides (DAGs), adducted as $[M+H]^+$, $[M + NH_4]^+$ and $[M+Na]^+$, while no monoglycerides were detected. Fourteen different DAGs were found, and interestingly, all of these species contained long-chain PUFA chains, such as C20:5, C22:4, C22:5, and C22:6. The distribution of DAGs in basa catfish and sole fish can be seen in the Fig. 3D, with sole fish exhibiting a higher content of long-chain polyunsaturated DAGs compared to basa catfish. The highest abundant species in sole fish were DAG(18:1/20:5), followed by DAG(18:0/22:6) and DAG(16:1/22:6). Basa catfish had fewer DAGs, with relatively higher abundances of DAG(16:0/22:4) and DAG(18:0/22:6), among others. TAGs were found to be the most diverse GL molecular species in both basa catfish and sole fish, with 278 and 294 species detected, respectively. TAGs are hydrolyzed by intestinal peristalsis and bile salt emulsification before being enzymatically cleaved within the intestinal lumen. The fatty acyl chains at the sn-1/3 positions are hydrolyzed into free fatty acids. The hydrolyzed 2-monoacylglycerides and free fatty acids are absorbed by intestinal epithelial cells, where they are resynthesized into new TAGs molecules. These TAGs are then

transported to the liver and adipose tissue via the lymphatic system and systemic circulation (Ye et al., 2019). Therefore, the identification of TAG molecules may contribute to understanding the beneficial effects of TAGs. The structure of TAGs varied in both fish tissue samples, depending on the carbon chain length and degree of unsaturation of the three fatty acid chains, resulting in different TAG molecular species through different arrangements. Several high-abundance TAG species contained fatty acid chains such as C16:0, C16:1, C18:0, C18:1, C20:5, and C22:6. Omega-3 PUFAs, such as DHA and EPA are essential fatty acids that cannot be synthesized by the human body. Calculation of the relative contents of EPA and DHA in the total TAG molecular species of basa catfish and sole fish was performed using peak area. As shown in Table 1, among the detected TAGs, basa catfish had 70 molecular species containing EPA or DHA, accounting for 5.9899% of the total TAGs, while sole fish had 86 molecular species containing EPA or DHA, accounting for 21.4160% of the total TAGs. There was a significant difference in the content of EPA or DHA in TAGs between the two fish species. The investigation reported by Wang et al. indicated that marine fish display elevated levels of PUFAs, which was consistent with our findings (Wang et al., 2019). The most abundant TAG molecules in two fish species were shown in Fig. 3C. In basa catfish, the highest content of TAGs included TAG(16:0/16:0/18:1), TAG(16:1/18:1/18:1), and TAG (16:0/16:1/18:1), which were mainly composed of fatty acyl chains such as C16:0, C16:1, and C18:1. In addition to the aforementioned TAGs, sole fish exhibited high levels of TAGs with fatty acyl chains such as C20:5, C22:5, and C22:6, such as TAG(16:0/16:1/20:5), TAG (16:0/20:5/22:5), and TAG(18:0/20:5/22:6). This variation could be attributed to the dietary habits of marine and freshwater fish. Marine fish primarily consume marine organism rich in EPA and DHA, such as zooplankton, crabs and shrimp etc., whereas freshwater fish predominantly feed on vegetation and plant material (Jabeen and Chaudhry, 2011).

Fatty acids are important metabolic energy sources and endogenous nutrients in fish during growth and development. A total of 20 free fatty acids were detected in basa catfish and sole fish, including 3 saturated fatty acids (SFA), 6 monounsaturated fatty acids (MUFA), and 11 PUFAs. The abundant of all fatty acid was displayed in heatmap (Fig. 3E). There were significant differences in the composition and relative content of free fatty acids between basa catfish and sole fish. The relative content of free SFA in basa catfish was 22.96%, free MUFA was 41.78%, and free PUFA was 35.26%, while in sole fish, the relative content of free SFA was 20.69%, free MUFA was 34.99%, and free PUFA was 44.32%. This finding aligned with prior literature, suggesting that marine fish exhibit higher concentrations of PUFA compared to freshwater fish (Gonçalves et al., 2021).

SPs, as important components of cell membranes, participate in biological processes such as cell growth, differentiation, and aging (Hannun and Obeid, 2018). The detected SPs in basa catfish and sole fish include sphingomyelin (SM), ceramide non-hydroxyfatty acid--dihydrosphingosine (Cer/NDS), ceramide non-hydroxyfatty acid--sphingosine (Cer/NS), hexosylceramide alpha-hydroxy fatty acid-phytospingosine (HexCer/AP), hexosylceramide non-hydroxyfatty acid-dihydrosphingosine (HexCer/NDS), hexosylceramide non-hydroxyfatty acid-hydrosphingosine (HexCer/NS), and sulfurhexosylceramide hydroxyfatty acid (SHexCer). The abundance of main SPs in two fish species were displayed in Fig. 3F. SM is composed of sphingosine (or neuroamine), fatty acids, phosphoric acid, and nitrogenous bases (Yang and Chen, 2022). Eleven types of SMs were detected in basa catfish and sole fish, with significant differences in the relative content of SM between the two fish species. Fifteen sulfur hexosylceramide (SHexCer) molecules were detected, all of which were predominantly long-chain structures ranging from C33 to C46 in length. Cer included Cer/NDS and Cer/NS, consisting of 11 and 18 molecules, respectively. High relative content Cer/NDS included Cer/NDS (d19:0/22:1) and Cer/NDS(d19:0/23:1), while high relative content Cer/NS included Cer/NS(d18:1/16:0), Cer/NS(d18:1/18:0), Cer/NS

Table 1
The relative abundance of TAG molecules containing EPA or DHA in the total TAGs in basa catfish and sole fish.

TAG molecules	Peak Area		Abundance (%) in total TAGs	
	Basa catfish	Sole fish	Basa catfish	Sole fish
TAG(12:0/12:0/22:6)	2.84E+07	5.14E+06	0.4018	0.0266
TAG(12:1/12:1/22:6)	8.64E+05	n.d	0.0122	n.d
TAG(12:2/12:2/22:6)	9.11E+07	1.03E+07	1.2887	0.0535
TAG(14:0/14:0/20:5)	1.73E+05	9.09E+06	0.0024	0.0470
TAG(14:0/15:0/20:5)	n.d	1.61E+07	n.d	0.0831
TAG(14:0/16:0/20:5)	1.93E+06	2.65E+08	0.0273	1.3716
TAG(14:0/16:0/22:6)	1.09E+07	2.71E+07	0.1536	0.1403
TAG(14:0/16:1/20:5)	1.28E+05	3.21E+07	0.0018	0.1662
TAG(14:0/16:1/22:6)	1.99E+05	5.67E+07	0.0028	0.2936
TAG(14:0/18:3/20:5)	1.44E+06	2.19E+06	0.0204	0.0113
TAG(14:0/20:4/20:5)	1.48E+04	3.16E+07	0.0002	0.1633
TAG(14:0/20:5/20:5)	1.23E+06	2.22E+07	0.0175	0.1146
TAG(14:0/20:5/22:6)	3.43E+04	8.22E+06	0.0005	0.0426
TAG(14:0/22:6/22:6)	n.d	1.59E+07	n.d	0.0822
TAG(15:0/16:1/20:5)	n.d	4.16E+07	n.d	0.2153
TAG(15:0/22:6/22:6)	n.d	1.02E+07	n.d	0.0527
TAG(16:0/16:0/20:5)	1.23E+07	1.30E+08	0.1736	0.6735
TAG(16:0/16:0/22:6)	1.01E+07	3.50E+07	0.1425	0.1809
TAG(16:0/16:1/20:5)	2.49E+06	4.94E+08	0.0352	2.5567
TAG(16:0/16:1/22:6)	5.98E+06	4.40E+08	0.0846	2.2774
TAG(16:0/17:0/22:6)	8.54E+06	3.47E+06	0.1208	0.0180
TAG(16:0/17:1/22:6)	1.10E+08	3.39E+07	1.5570	0.1754
TAG(16:0/18:1/20:5)	n.d	5.04E+05	n.d	0.0026
TAG(16:0/18:1/22:6)	1.56E+06	7.60E+06	0.0220	0.0393
TAG(16:0/18:2/22:6)	4.89E+06	2.24E+08	0.0691	1.1607
TAG(16:0/20:4/20:5)	3.62E+05	1.19E+08	0.0051	0.6157
TAG(16:0/20:5/20:5)	6.34E+05	2.19E+07	0.0090	0.1133
TAG(16:0/20:5/21:0)	8.81E+05	6.49E+06	0.0125	0.0336
TAG(16:0/20:5/21:5)	1.74E+06	2.72E+07	0.0246	0.1410
TAG(16:0/20:5/22:5)	4.85E+05	2.84E+08	0.0069	1.4675
TAG(16:0/20:5/22:6)	6.15E+05	3.85E+07	0.0087	0.1992
TAG(16:0/22:1/22:6)	1.09E+07	1.74E+08	0.1547	0.9000
TAG(16:0/22:5/22:6)	1.88E+05	2.85E+07	0.0027	0.1475
TAG(16:1/16:1/20:5)	6.01E+05	5.82E+07	0.0085	0.3012
TAG(16:1/16:1/22:6)	5.98E+05	4.62E+07	0.0085	0.2390
TAG(16:1/17:1/20:5)	9.31E+06	6.06E+06	0.1318	0.0314
TAG(16:1/17:1/22:6)	1.11E+06	8.94E+05	0.0157	0.0046
TAG(16:1/17:2/22:6)	1.30E+06	3.67E+04	0.0184	0.0002
TAG(16:1/20:4/20:5)	3.16E+04	1.36E+05	0.0004	0.0007
TAG(16:1/20:5/20:5)	4.97E+05	1.46E+07	0.0070	0.0756
TAG(16:1/20:5/22:5)	n.d	4.76E+06	n.d	0.0246
TAG(16:1/20:5/22:6)	3.19E+04	1.53E+07	0.0005	0.0792
TAG(16:1/22:5/22:6)	6.22E+05	1.42E+08	0.0088	0.7366
TAG(16:1/22:6/22:6)	1.52E+04	1.38E+07	0.0002	0.0714
TAG(16:2/22:6/22:6)	2.56E+05	7.17E+06	0.0036	0.0371
TAG(17:0/18:0/22:6)	4.60E+05	1.81E+06	0.0065	0.0094
TAG(17:0/18:1/22:6)	n.d	1.39E+07	n.d	0.0720
TAG(17:0/20:4/20:5)	7.43E+05	6.67E+05	0.0105	0.0035
TAG(17:0/20:5/20:5)	n.d	1.45E+07	n.d	0.0751
TAG(17:0/20:5/22:5)	n.d	6.61E+07	n.d	0.3420
TAG(17:0/20:5/22:6)	1.11E+07	7.18E+07	0.1574	0.3717
TAG(17:0/22:1/22:6)	1.19E+05	2.08E+07	0.0017	0.1075
TAG(17:0/22:5/22:6)	n.d	5.11E+07	n.d	0.2643
TAG(17:0/22:6/22:6)	1.84E+06	2.02E+07	0.0260	0.1044
TAG(17:1/17:1/22:6)	3.85E+05	2.35E+06	0.0054	0.0122
TAG(17:1/18:0/22:6)	1.67E+06	n.d	0.0236	n.d
TAG(17:1/18:1/22:6)	7.64E+04	4.37E+07	0.0011	0.2261
TAG(17:1/20:5/22:6)	4.22E+06	9.44E+06	0.0597	0.0488
TAG(17:2/17:2/20:5)	3.39E+06	3.92E+07	0.0480	0.2031
TAG(18:0/18:0/20:5)	3.91E+07	6.53E+07	0.5529	0.3380
TAG(18:0/18:0/22:6)	1.30E+06	1.37E+07	0.0184	0.0708
TAG(18:0/19:0/22:6)	3.77E+06	2.64E+07	0.0534	0.1368
TAG(18:0/20:5/20:5)	9.32E+05	1.32E+05	0.0132	0.0007
TAG(18:0/20:5/22:6)	9.11E+05	3.33E+08	0.0129	1.7248
TAG(18:0/22:5/22:6)	3.39E+04	4.26E+07	0.0005	0.2206
TAG(18:0/22:6/22:6)	n.d	2.26E+05	n.d	0.0012
TAG(18:1/18:1/20:5)	1.62E+06	9.90E+06	0.0229	0.0512
TAG(18:1/18:1/22:6)	1.92E+07	3.95E+07	0.2722	0.2041
TAG(18:1/19:0/22:6)	1.81E+05	3.89E+07	0.0026	0.2015
TAG(18:1/20:1/20:1)	7.20E+05	4.31E+06	0.0102	0.0223
TAG(18:1/20:1/22:6)	3.77E+06	7.46E+07	0.0534	0.3861
TAG(18:1/20:4/20:5)	9.34E+04	9.10E+06	0.0013	0.0471

(*continued on next page*)

Table 1 (*continued*)

TAG molecules	Peak Area		Abundance (%) in total TAGs	
	Basa catfish	Sole fish	Basa catfish	Sole fish
TAG(18:1/20:5/20:5)	8.14E+04	5.50E+06	0.0012	0.0285
TAG(18:1/22:5/22:6)	4.42E+04	5.81E+07	0.0006	0.3004
TAG(18:1/22:6/22:6)	3.51E+05	1.16E+07	0.0050	0.0601
TAG(18:2/20:5/20:5)	1.77E+05	3.23E+07	0.0025	0.1671
TAG(19:1/19:1/22:6)	2.99E+06	2.83E+07	0.0423	0.1462
TAG(20:0/20:0/20:5)	1.04E+05	9.03E+06	0.0015	0.0467
TAG(20:1/20:1/22:6)	n.d	3.40E+06	n.d	0.0176
TAG(20:1/20:5/20:5)	1.44E+06	1.44E+05	0.0204	0.0007
TAG(20:4/22:5/22:6)	n.d	8.09E+06	n.d	0.0419
TAG(20:4/22:6/22:6)	n.d	8.26E+06	n.d	0.0428
TAG(20:5/20:5/20:5)	1.18E+04	4.41E+06	0.0002	0.0228
TAG(20:5/20:5/22:6)	n.d	4.17E+06	n.d	0.0216
TAG(20:5/22:5/22:6)	n.d	9.03E+05	n.d	0.0047
TAG(20:5/22:6/22:6)	n.d	6.43E+06	n.d	0.0333
TAG(21:1/21:1/22:6)	5.50E+04	1.02E+07	0.0008	0.0527
TAG(22:5/22:6/22:6)	n.d	3.07E+06	n.d	0.0159
Total			5.9899	21.4160

Note: n.d.: not detected.

(d18:1/22:0), Cer/NS(d18:1/22:1), and Cer/NS(d18:1/24:1), among others. HexCer in basa catfish and sole fish consisted of 3 major classes: HexCer/AP, HexCer/NDS, and HexCer/NS, encompassing 3, 4, and 4 different molecular species, respectively. Basa catfish had fewer HexCer molecular species, mainly including HexCer/NDS(d18:0/24:2) and HexCer/NS(d14:2/26:0), while sole fish exhibited a more abundant presence of HexCer, essentially containing various HexCer molecular species mentioned above. Additionally, 6 Acar, 5 AcylGlcADG, and 6 GlcADG were observed, referring to the Table S2 for specific molecular information.

3.3. Statistical analysis

Chemometrics was further applied to analyze the differences in lipid composition between the two fish species. The substantial matrix dataset encompassing 779 feature ions and 32 samples (2 fish species × 16 parallels) were imported into SIMCA-P software for PCA and OPLS-DA modeling. The objective was to differentiate basa catfish from sole fish and identify the characteristic lipid molecules contributing to the observed differences. Prior to conducting principal component analysis (PCA), the lipid data were normalized to reduce any biases introduced during sample collection and lipid extraction processes. PCA, as an unsupervised method, performs dimensionality reduction and data transformation on the pre-processed data, with the resultant feature vectors representing the principal components (Granato et al., 2018). From the PCA score plot (Fig. 4A), it can be observed that samples of basa catfish and sole fish form two distinct and statistically significant clusters, indicating noticeable differences between the two sample groups. The percentage variance explained by the first two principal components (PC1 and PC2) was calculated as 93.558 cum%, with PC1 (R2X[1]) explaining 93 cum% (R2X[1]) and PC2 explaining 0.558 cum% (R2X[2]), indicating good explanatory power. In Fig. 4B, all the sample data points fell below the 95% confidence limit, without any outliers, suggesting a well-performed and reliable model suitable for species discrimination.

To identify lipid biomarkers distinguishing basa catfish from sole fish, an OPLS-DA model was constructed for species comparison. OPLS-DA, built upon the PLS-DA algorithm, filters out "noise" variables in X data that are unrelated to the predictive variable Y (Liu et al., 2024). To assess whether the current OPLS-DA model was overfitting, a permutation test was conducted on the basa catfish samples, repeated 200 times. In the OPLS-DA model, the R^2 and Q^2 values reflect the model's

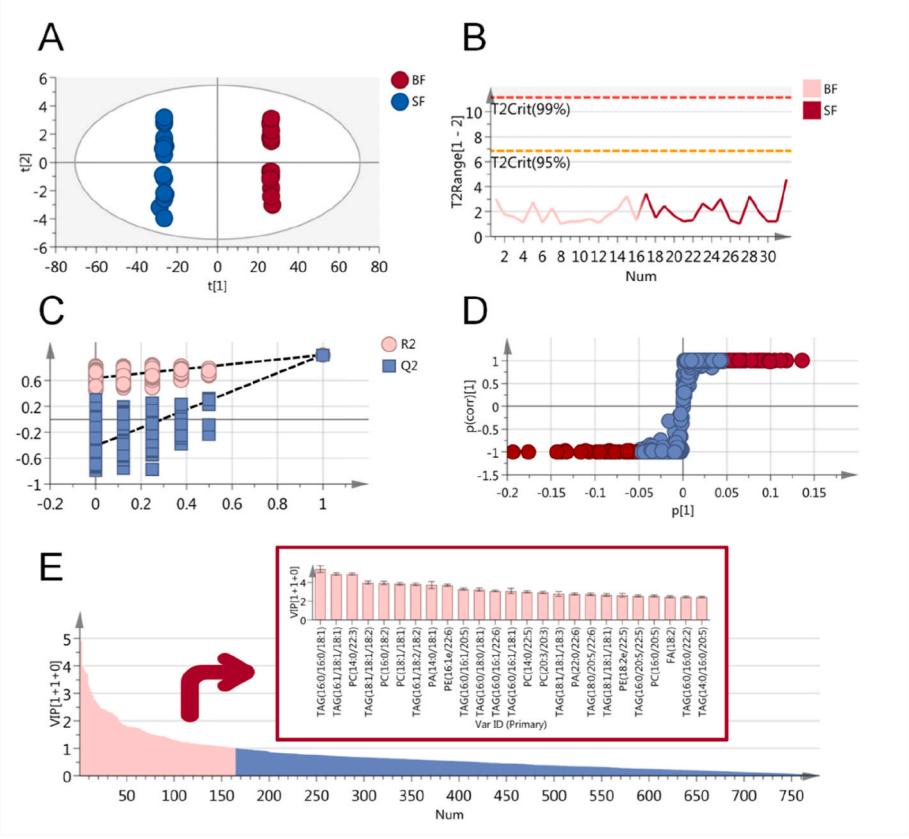

Fig. 4. Multivariate statistical analysis plot of all detected lipid molecular species in basa catfish and sole fish: Score plots of PCA model (A), the hoteling's T2 plot of PCA (B), the permutation test plot (C), the S-plot (D) and the VIP plot (E).

explanatory power and predictive ability. The intercept values of R^2 and Q^2 were 0.622 and −0.423, respectively (Fig. 4C), with all the left-side permutation values lower than the right-side original values, indicating the reliability of the OPLS-DA model without overfitting and its suitability for assessing differences between sample groups. The S-plot visually displays the observed variables on a two-dimensional plane, particularly highlighting the compounds located on the "S" wings, which represent the most significant differences between the two groups and hold high research value. Variables with $|p| \geq 0.05$ and $|p(corr)| \geq 0.5$ are considered statistically significant (Zhao et al., 2020). From Fig. 4D, it can be observed that |p| and |p(corr)| values of TAG (16:1/20:4/20:5), PE(22:6/22:6), and TAG(14:0/20:5/22:6) were relatively high, suggesting their significant contributions to differentiating basa catfish from sole fish. Using a VIP threshold >1 for screening differential lipids (Fig. 4E) (Chung et al., 2019), 614 lipid species were excluded, leaving 165 potential biomarkers. These included 89 TAGs, 19 PCs, 16 PEs, 11 PAs, 10 PGs, 8 PSs, 4 PIs, 4 FAs, 1 SHexCer, 1 GlcADG, and 2 Cer/NS. The top 25 ions with the highest VIP values are highlighted in Fig. 4E, such as TAG(16:0/16:0/18:1), TAG(16:1/18:1/18:1) and PC(14:0/22:3), etc. These lipid molecules represent the most important differentiating factors between basa catfish and sole fish, serving as potential identification markers for these two fish species.

4. Conclusions

This study employed the advanced UHPLC-QE Orbitrap MS technology to elucidate the lipid composition of basa catfish and sole fish. A total of 779 lipid molecules across various lipid classes were identified in positive and negative ion modes, with phospholipids and glycerolipids dominating. As a marine fish, sole fish exhibited a structure with more polyunsaturated PLs, DAGs and TAGs, such as PC(16:0/20:5), PC(16:0/22:6), DAG(18:1/20:5), DAG(18:0/22:6), TAG(16:0/16:1/20:5), TAG (16:0/20:5/22:5), etc. Furthermore, the authentication of two fish samples was achieved through the analysis of their lipid profiles using multivariate statistical analysis. This study revealed significant differences in the lipid fingerprints between the two fish species. TAG(16:0/16:0/18:1), PC(14:0/22:3), and TAG(16:1/18:1/18:1), etc. were identified as the primary ions contributing to the distinction between the two fish samples. This study not only highlighted the potential of lipidomics in distinguishing various fish species but also underscored its significance in nutritional studies. The findings implied that further exploration of the nutritional values of these lipids could lead to novel insights into the health benefits and dietary applications of different fish species.

Credit author statement

Weibo Lu: Investigation, Writing, Validation. **Yunyan Li**: Methodology, Writing. **Ge Lijun**: Methodology. **Honghai Wang**: Revision. **Ting Liu:** Investigation, Software. **Qiaoling Zhao**: Validation. **Zhujun Mao:** Revision. **Jingjing Liang:** Statistics, Revision. **Pingya Wang:** Data curation. **Kang Chen:** Data curation. **Jing Xue:** Conceptualization, Revision. **Qing Shen**: Methodology, Revision, Funding acquisition.

Declaration of competing interest

The authors declare that they have no known competing financial interests or personal relationships that could have appeared to influence the work reported in this paper.

Data availability

No data was used for the research described in the article.

Acknowledgements

The authors thank the National Natural Science Foundation of China (32172304), Zhejiang Basic Public Welfare Research Project (LTGN24C200014), State Administration for Market Regulation Science and Technology Project (2023MK059), Eyas Program Incubation Project of Zhejiang Provincial Administration for Market Regulation (CY2022232), and Science and Technology Plan of Zhejiang Drug Administration (2021007)

Appendix A. Supplementary data

Supplementary data to this article can be found online at https://doi.org/10.1016/j.crfs.2024.100812.

References

Bellot, P.E.N.R., Moia, M.N., Reis, B.Z., Pedrosa, L.F.C., Tasic, L., Barbosa Jr, F., Sena-Evangelista, K.C.M., 2023. Are phosphatidylcholine and lysophosphatidylcholine body levels potentially reliable biomarkers in obesity? A review of human studies. Mol. Nutr. Food Res. 67 (7), 2200568.
Böhme, K., Calo-Mata, P., Barros-Velázquez, J., Ortea, I., 2019. Recent applications of omics-based technologies to main topics in food authentication. Trac-trend Anal Chem. 110, 221–232.
Bosko, S.A., Foley, D.M., Hellberg, R.S., 2018. Species substitution and country of origin mislabeling of catfish products on the U.S. commercial market. Aquaculture 495, 715–720.
Chang, C.-H., Tsai, M.-L., Huang, T.-T., Wang, Y.-C., 2021. Authentication of fish species served in conveyor-belt sushi restaurants in Taiwan using DNA barcoding. Food Control 130, 108264.
Chung, I.-M., Kim, J.-K., Han, J.-G., Kong, W.-S., Kim, S.-Y., Yang, Y.-J., An, Y.-J., Kwon, C., Chi, H.-Y., Yhung Jung, M., Kim, S.-H., 2019. Potential geo-discriminative tools to trace the origins of the dried slices of shiitake (Lentinula edodes) using stable isotope ratios and OPLS-DA. Food Chem. 295, 505–513.
Dai, X., Shen, L., 2022. Advances and trends in omics technology development. Front. Med. 9.
Dai, Y., Yuan, Y.-M., Yuan, Y., Zhou, Z., Zhang, H., 2022. Factors influencing Chinese consumer attitudes on the safety of aquatic products. J. World Aquacult. Soc. 53 (1), 47–59.
Deng, J., Yang, Y., Luo, L., Xiao, Y., Luan, T., 2020. Lipid analysis and lipidomics investigation by ambient mass spectrometry. Trac-trend Anal Chem. 128, 115924.
Engel, K.M., Prabutzki, P., Leopold, J., Nimptsch, A., Lemmnitzer, K., Vos, D.R.N., Hopf, C., Schiller, J., 2022. A new update of MALDI-TOF mass spectrometry in lipid research. Prog. Lipid Res. 86, 101145.
Gonçalves, R.M., Petenuci, M.E., Maistrovicz, F.C., Galuch, M.B., Montanher, P.F., Pizzo, J.S., Gualda, I.P., Visentainer, J.V., 2021. Lipid profile and fatty acid composition of marine fish species from Northeast coast of Brazil. J. Food Sci. Technol. 58 (3), 1177–1189.
Granato, D., Santos, J.S., Escher, G.B., Ferreira, B.L., Maggio, R.M., 2018. Use of principal component analysis (PCA) and hierarchical cluster analysis (HCA) for multivariate association between bioactive compounds and functional properties in foods: a critical perspective. Trends Food Sci. Technol. 72, 83–90.
Hachem, M., Nacir, H., 2022. Emerging role of phospholipids and lysophospholipids for improving brain docosahexaenoic acid as potential preventive and therapeutic strategies for neurological diseases. Int. J. Mol. Sci. 23 (7), 7.
Hannun, Y.A., Obeid, L.M., 2018. Sphingolipids and their metabolism in physiology and disease. Nat. Rev. Mol. Cell Biol. 19 (3), 175–191.
Hassoun, A., Måge, I., Schmidt, W.F., Temiz, H.T., Li, L., Kim, H.-Y., Nilsen, H., Biancolillo, A., Aït-Kaddour, A., Sikorski, M., Sikorska, E., Grassi, S., Cozzolino, D., 2020. Fraud in animal origin food products: advances in emerging spectroscopic detection methods over the past five years. Foods 9 (8), 1069.
Innes, J.K., Calder, P.C., 2020. Marine omega-3 (N-3) fatty acids for cardiovascular health: an update for 2020. Int. J. Mol. Sci. 21 (4), 1362.
Jabeen, F., Chaudhry, A.S., 2011. Chemical compositions and fatty acid profiles of three freshwater fish species. Food Chem. 125 (3), 991–996.
Khor, Y.P., Wan, S.Y., Tan, C.P., Zhao, G., Li, C., Wang, Y., Li, Y., 2021. Potential of using basa catfish oil as a promising alternative deep-frying medium: a thermo-oxidative stability study. Food Res. Int. 141, 109897.
Law, S.-H., Chan, M.-L., Marathe, G.K., Parveen, F., Chen, C.-H., Ke, L.-Y., 2019. An updated review of lysophosphatidylcholine metabolism in human diseases. Int. J. Mol. Sci. 20 (5), 1149.
Li, Q., Zhao, Y., Zhu, D., Pang, X., Liu, Y., Frew, R., Chen, G., 2017. Lipidomics profiling of goat milk, soymilk and bovine milk by UPLC-Q-Exactive Orbitrap Mass Spectrometry. Food Chem. 224, 302–309.
Liu, M., Yang, Y., Zhao, X., Wang, Y., Li, M., Wang, Y., Tian, M., Zhou, J., 2024. Classification and characterization on sorghums based on HS-GC-IMS combined with OPLS-DA and GA-PLS. Curr. Res. Food Sci. 8, 100692.
Ma, J., Li, T., Chen, H., Wang, C., Wang, H., Li, Q., 2021. Lipidomic analysis and diagnosis of glioblastoma multiforme with rapid evaporative ionization mass spectrometry. Electrophoresis 42 (19), 1965–1973.
Matyash, V., Liebisch, G., Kurzchalia, T.V., Shevchenko, A., Schwudke, D., 2008. Lipid extraction by methyl-tert-butyl ether for high-throughput lipidomics. J. Lipid Res. 49 (5), 1137–1146.

Navarro-Reig, M., Jaumot, J., Tauler, R., 2018. An untargeted lipidomic strategy combining comprehensive two-dimensional liquid chromatography and chemometric analysis. J. Chromatogr. A 1568, 80–90.
Rey, F., Melo, T., Lopes, D., Couto, D., Marques, F., Domingues, M.R., 2022. Applications of lipidomics in marine organisms: progress, challenges and future perspectives. Mol. Omics 18 (5), 357–386.
Stoica, C., Ferreira, A.K., Hannan, K., Bakovic, M., 2022. Bilayer forming phospholipids as targets for cancer therapy. Int. J. Mol. Sci. 23 (9). Article 9.
Shahidi, F., Ambigaipalan, P., 2018. Omega-3 polyunsaturated fatty acids and their health benefits. Annu. Rev. Food Sci. Technol. 9 (1), 345–381.
Sriket, P., La-ongnual, T., 2018. Quality changes and discoloration of basa (*Pangasius bocourti*) fillet during frozen storage. J. Chem. 2018, e5159080.
Tietel, Z., Hammann, S., Meckelmann, S.W., Ziv, C., Pauling, J.K., Wölk, M., Würf, V., Alves, E., Neves, B., Domingues, M.R., 2023. An overview of food lipids toward food lipidomics. Compr. Rev. Food Sci. Food Saf. 22 (6), 4302–4354.
Wang, D., Hsieh, Y.-H.P., 2016. The use of imported pangasius fish in local restaurants. Food Control 65, 136–142.
Wang, X., Zhang, H., Song, Y., Cong, P., Li, Z., Xu, J., Xue, C., 2019. Comparative lipid profile analysis of four fish species by ultraperformance liquid chromatography coupled with quadrupole time-of-flight mass spectrometry. J. Agric. Food Chem. 67 (33), 9423–9431.
Xuan, Q., Hu, C., Yu, D., Wang, L., Zhou, Y., Zhao, X., Li, Q., Hou, X., Xu, G., 2018. Development of a high coverage pseudotargeted lipidomics method based on ultra-high performance liquid chromatography–mass spectrometry. Anal. Chem. 90 (12), 7608–7616.
Yang, F., Chen, G., 2022. The nutritional functions of dietary sphingomyelin and its applications in food. Front. Nutr. 9.
Ye, Z., Li, R., Cao, C., Xu, Y.-J., Cao, P., Li, Q., Liu, Y., 2019. Fatty acid profiles of typical dietary lipids after gastrointestinal digestion and absorbtion: a combination study between in-vitro and in-vivo. Food Chem. 280, 34–44.
Zhao, S., Liu, H., Su, Z., Khoo, C., Gu, L., 2020. Identifying cranberry juice consumers with predictive OPLS-DA models of plasma metabolome and validation of cranberry juice intake biomarkers in a double-blinded, randomized, placebo-controlled, cross-over study. Mol. Nutr. Food Res. 64 (11), 1901242.
Zink, K.-G., Mangelsdorf, K., 2004. Efficient and rapid method for extraction of intact phospholipids from sediments combined with molecular structure elucidation using LC–ESI-MS–MS analysis. Anal. Bioanal. Chem. 380 (5), 798–812.